LEP Note 459
and PS/LPI/ Note 83 - 9
29.06.1983

LEP/LIBRARY

PARTICLE TRACKING IN THE EPA BENDING MAGNET

M. Bell - J.P. Delahaye

I - INTRODUCTION

The bending magnet is obviously the main element of the EPA lattice [1]. Responsible not only for the closed orbit deflection but also for the strength and for the repartition of damping, it moreover contributes to the vertical beam focussing and to the appropriate shaping of the dispersion function. In consequence, many of the EPA parameters depend on the characteristics of the bending magnet. The hard edge approximation with which they have until now been deduced has been deemed insufficient because of the specificity of the very low bending radius in a specially short combined function magnet.

It's the reason why precise particle tracking based on accurate magnetic field estimations [2] has been initiated in order to deduce the exact bending magnet properties.

The bending magnet characteristics (length - pole profile) have then been reviewed in order to match better the beam dynamics constraints.

Finally the EPA lattice had been reoptimized and the consequent ring and beam parameters recalculated.

II - Main tasks of the EPA bending magnet :

The very important tasks devoted to the bending magnet imposes the accurate knowledge of not only the particle trajectories but also of the different synchrotrons integrals along the trajectory as well as of the equivalent transfer matrix.

II.1. The high deflection angle required ($\theta = 22^{\circ}\ 5$) necessitates a big and precise bending strength [3].

$$\int B\, d\ell = 7854 \pm 4 \text{ gm } (\pm 5 \times 10^{-4})$$

./.

II.2. A high damping rate $1/\tau_i$, very beneficial to the accumulation process, is provided by a magnetic field at the limit of saturation[4] :
$B_o = 1.4$ T

In fact, $\tau_i \alpha \frac{I_2}{Ji} = \frac{B^2 ds}{Ji}$

where I_2 is the second synchrotron integral
Ji is the damping partition number in the plane i.

That is the reason for a magnet with a very short length ($\ell m = 0.56$ m) and bending radius ($\rho = 1{,}43$ m)

II.3. An exchange of the horizontal and longitudinal damping partition numbers J_x, favours the injection efficiency as well as the beam stability[1].

$$J_x = 1 - I_4/I_2$$

where $I_4 = \left[B^3 (s) + 2 B (s) G (s)\right] D x \, ds$

That is the reason for the introduction of a small defocussing gradient in the magnet :

$$J_x \sim 2 \Leftrightarrow G \simeq \frac{dBy}{dx} \sim -1 \text{ T/m}$$

II.4. Taking advantage of its vertical focussing strength, the bending magnet is used as a D quadrupole in the curved part of the EPA lattice based on a quadruplet FDDF structure. Moreover, the contribution to the focussing of the fringe field $(k\ell)_{ff}$ cannot be neglected[5] because of the specially low bending radius.
In the case of a pure dipole magnet :

$$(k\ell)_{ff} = \left(\frac{1 + \sin^2\varepsilon}{\rho^2 \cos \varepsilon}\right) \int \frac{B(s) \left[B_o - B(s)\right]}{B_o^2} ds$$

where ε is the angle between trajectory and bending faces.
B_o is the magnetic field in the center of the magnet.

./.

II.5. A sextupolar strength in the bending magnet first envisaged for chromaticity correction has finally been removed for two reasons : first, the non-linearities so introduced in half of the magnets are unefficient for chromaticity correction because of their dispersion free situation and decrease substancially the dynamic aperture[6].

secondly, as pointed out by A. Krusche, the presence of a sextupole field in the magnet would notably change the bending and focussing strength along the trajectory because of its specially low bending radius (Annex 1).

III - First approximation of the beam behaviour in the bending magnet

In the particular case of a specially short bending magnet affected by a very low bending radius together with a combined function, the magnetic field and its gradient are varying in all directions all along the trajectory. Unfortunately the analytical integration of the exact equation of motion is not possible in this very general case (Annex 2).

This is the reason why the bending magnet behaviour was first deduced from an approximation based on a magnet split in three parts.

III.1. Central part in the hard edge approximation (B and G constants)

The bending and focussing strength along the trajectory are then calculated as if the closed orbit stayed on the magnet axis. This procedure is completely right for the focussing in the absence of sextupole (Annex 1) but is not for the bending strength because of the presence of the gradient and because of the lengthening of the trajectory.

The equivalent gradient magnetic length, l_G, is estimated[7] from the equivalent bending magnetic length, l_B.

$$\ell_G = \ell_B + \frac{Bo}{(dB/dx)o} \frac{dl_B}{dx}$$

In the EPA case, this difference reaches 60 mm ($\sim$ 11 %)

The synchrotrons integrals evaluated along the trajectory are surestimated as :

$$\int B(s)^n ds < B_o{}^n \int ds$$

III.2. Edge part where the magnetic field and gradient vary suddenly

This results in a well known equivalent vertically focussing quadrupole of strength $\frac{1}{f}$ tg ε. The corresponding angle ε between bending faces and central trajectory has first to be corrected by the variation of the magnetic length with the horizontal position. ("Slant" magnet)

$$\varepsilon = \frac{1}{2}\left(\theta - \frac{dl_B}{dx}\right)$$

This variation can be approximated by[8]

$$\frac{dl_B}{dx} \sim 1.3\,\frac{dg}{dx}$$

where g is the magnet gap.

In the EPA case : $\frac{dg}{dx} = \frac{0.52}{28} \Rightarrow \frac{dl_B}{dx} = 0.048 \Rightarrow \Delta\varepsilon \sim 25$ mrad

III.3. Fringe field extension :

This part is obviously the more difficult to treat accurately.
First because the variations of the gradient in the fringe field is certainly different from the magnetic field variation.
Secondly because the corresponding vertical focussing already mentioned is only an approximation up to the second order in $\frac{1}{f}$.

./.

IV. Exact particle Tracking

In order to remove all these different approximations, a precise particle tracking based on exact particle equation of movement (Annex II) has been launched.

It uses magnetic field estimations[2] deduced from two dimensional computer programs whose results have been first checked by comparison with magnetic measurements on a very similar bending magnet[9].

The main tasks of this particle tracking was :

a) to calculate the position of the central trajectory through the whole magnet including the fringe field extension.

b) to adjust the total length of the magnet in order to fit the desired deflection angle of $\theta = 392{,}7$ mrad.

c) to determine the exact synchrotrons integrals all along the central trajectory from the known values of the magnetic fields and of its gradient assuming the dispersion and the H function from the AGS linear optic program[10].

$$I_1 = \oint \frac{D(s)}{\rho(s)}\,ds = \frac{\langle D\rangle}{(B_0\rho_0)}\oint B(s)\,ds$$

$$I_2 = \oint \frac{ds}{\rho^2(s)} = \frac{1}{(B_0\rho_0)^2}\oint B^2(s)\,ds$$

$$I_3 = \oint \frac{ds}{\rho^3(s)} = \frac{1}{(B_0\rho_0)^3}\oint B^3(s)\,ds$$

$$I_4 = \oint \frac{(1-2n)D(s)}{\rho^3(s)}\,ds = \frac{\langle D\rangle}{(B_0\rho_0)^3}\oint\left[B^3(s) + 2(B_0\rho_0)B(s)\frac{dB(s)}{d\eta}\right]ds$$

$$I_5 = \oint \frac{H(s)}{\rho^3(s)}\,ds = \langle H\rangle\, I_3$$

with $\langle D\rangle$ the mean value of the dispersion function in the magnets

$\langle H\rangle$ the mean value of the function H in the magnet.

$$H(s) = \frac{R^2}{\beta(s)}\left[D^2(s) + \left(\beta(s)D'(s) - \frac{1}{2}\beta'(s)D(s)\right)^2\right]$$

./.

d) to deduce the exact equivalent transfer matrix $[H]$, $[V]$ respectively in horizontal and vertical plane by tracking particle slightly deviated from the central orbit and comparison between the entry (1) an exit (2) of the magnet

$$H_{11} = \frac{\Delta \eta_2}{\Delta \eta_1} \qquad V_{11} = \frac{\Delta y_2}{\Delta y_1}$$

$$H_{12} = \frac{\Delta \eta_2}{\Delta \eta'_1} \qquad V_{12} = \frac{\Delta y_2}{\Delta y'_1}$$

$$H_{21} = \frac{\Delta \eta'_2}{\Delta \eta_1} \qquad V_{21} = \frac{\Delta y'_2}{\Delta y_1}$$

$$H_{22} = \frac{\Delta \eta'_2}{\Delta \eta'_1} \qquad V_{22} = \frac{\Delta y'_2}{\Delta y'_1}$$

$$H_{13} = \frac{\Delta \eta_2}{\Delta p/p} \qquad V_{13} = \frac{\Delta \eta'_2}{\Delta p/p}$$

where η and η' are the horizontal position and slope in the direction perpendicular to the trajectory.

e) to adjust the internal gradient in the magnet in order that the corresponding transfer matrix perturbs as little as possible the EPA lattice.
This perturbation has been calculated by a new version of the linear optic computer program AGS[10] specially modified by T. Risselada in order to be able to replace any element by its numerical equivalent transfer matrix.

./.

V. EPA bending magnet and lattice modifications

After different field configuration calculations (Fig. 1) a new set of characteristics for the EPA bending magnet (Table 1) have been decided for a minimum of perturbation of the main lattice parameters (Fig. 2) :

The main modification consists in a 12 % increase of the internal gradient to compensate the loss in focussing by the edges due to the varying magnetic length with horizontal position.

The corresponding central orbit position has then been deduced as well as the different bending and focussing strength along the central trajectory and the straight magnet axis (Fig. 3).

The equivalent transfer matrix and the real synchrotrons integrals have after that been evaluated and compared to the hard edge approximation results (Table 1).

Finally the lattice has been reoptimized using in place of the bending magnet the above equivalent transfer matrix.

The same lattice parameters (β and dispersion functions, phase advances betatron working point, transition energy) have been found again (cf. Table 2 : Listing AGS annexed) by slightly adjusting the strength of the main lattice quadrupoles (some % change) as well as of the little trim quadrupoles HR.QTR ($\sim$ 170 g) already needed for the energy range operation[5].

VI. Beam dynamics modifications :

All beam dynamics parameters relevant to the synchrotron integrals will consequently be modified.
It concerns specially the energy loss per turn, the damping partition numbers and damping time constants, and therefore the beam emittances at injection as well as at equilibrium. They are summarized together with their "old" value in Table 1.

./.

VI.1. Energy loss per turn : U_γ

This parameter will be slightly decreased according to the second synchrotron integral change (-10 %)

$$U_\gamma(\text{keV}) = 14.08.\ I_2.\ E^4\ (\text{GeV})$$

$$\left.\begin{array}{l} I_2 = 3.95 \\ E = 0.6\ \text{GeV} \end{array}\right\} \Longrightarrow \quad U_\gamma = 7.21\ \text{keV}$$

VI.2. Stable phase angle during accumulation : φ_s

Keeping the total V_{RF} voltage to 50 kV for the linac momentum acceptance of ± 1.2 %

$$\varphi_s = \text{Arc sin.}\ (U_\gamma / V_{RF})$$

$$\left.\begin{array}{l} U_\gamma = 7.21\ \text{keV} \\ V_{RF} = 50\ \text{kV} \end{array}\right\} \Longrightarrow \quad \varphi_s = 171.7^\circ$$

VI.3. Damping partition numbers : Ji

Due to a nearly same decrease of both the second and fourth synchrotron integrals, these parameters are little perturbed :

$$J_x = 1 - I_4/I_2 \ ; \ J_y = 1 \ ; \ J_\varepsilon = 2 + I_4/I_2$$

$$\left.\begin{array}{l} I_2 = 3.95 \\ I_4 = -3.98 \end{array}\right\} \Longrightarrow \left\{\begin{array}{l} J_x = 2.01 \\ J_\varepsilon = 0.99 \end{array}\right.$$

VI.4. Damping time constants : τ_i

The damping time constants suffer from a substantial increase of up to 16 % for the longitudinal one

$$\tau_i = \frac{2.976 \times 10^{24}\ R}{I_2\ J_i\ E}$$

τ_x = 34.71 msec. τ_y = 69.77 msec. τ_ε = 70.47 msec.

./.

VI.5. Beam emittance after injection : ε_T

This very important parameter from which depend the vacuum chamber dimension increases by some 4 % because of the smaller horizontal damping. Moreover another 6 % increase is due to the widening by 1 mm of the injection septum apparent width, S, [11].

$$S = 10 \text{ mm} \qquad \varepsilon_T = 112\ \pi \text{ mm-mrad}$$

$$S = 11 \text{ mm} \qquad \varepsilon_T = 119\ \pi \text{ mm-mrad}$$

The beam enveloppe at injection is nevertheless only slightly modified and does not affect the vacuum chambers dimensions.

VI.6. Beam emittances at equilibrium : ε_{xo} , ε_{yo}

The equivalent decrease of the second and fifth synchrotron integrals limits the modification of the equilibrium beam emittances.

$$\underset{(1\ \sigma)}{\varepsilon_{xo}} = 1.47 \times 10^{-24}\ \frac{I_5}{J_x\, I_2}\ E_2^{\,2}$$

$$\left.\begin{aligned} I_2 &= 3.95 \\ I_S &= 2.02 \end{aligned}\right\} \Longrightarrow \quad \varepsilon_{xo} = 0.135\ \pi \text{ mm-mrad}$$

Assuming a maximum coupling $\mathcal{K}$ of 25 % between the two transverse planes :

$$\varepsilon_{zo} = \frac{\mathcal{K}}{1+\mathcal{K}}\ \varepsilon_{xo}$$

$$\mathcal{K} = 0{,}25 \qquad \Longrightarrow \qquad \underset{(1\ \sigma)}{\varepsilon_{zo}} = 0{,}027\ \pi \text{ mm-rmad}$$

VI.7. Momentum dispersion and length of the equilibrium beam : σ_E/E ; σ_{so}

Here also, the equivalent decrease of the second and third synchrotron integrals reduces the equilibrium momentum dispersion change and therefore slightly affects the equilibrium bunch length σ_{so}

$$\frac{\sigma_E}{E} = \pm 1{,}21.10^{-12}\left(\frac{I_3}{J_\varepsilon\ I_2}\right)^{1/2} E$$

$$\left.\begin{array}{l} I_2 = 3{,}95 \\ I_3 = 2{,}64 \end{array}\right\} \Longrightarrow \frac{\sigma_E}{E} \pm 5{,}96.10^{-4}$$

$$\sigma_{so}\ (1\ \sigma) = 2{,}506\ \frac{R}{\gamma_{tr}}\left(\frac{E}{hqV_{RF}\cos\varphi_s}\right)^{1/2}\left(\frac{\sigma_E}{E}\right)$$

$$\left.\begin{array}{l} \sigma_{E/E} = 5{,}96.10^{-4} \\ \gamma_{tr} = 5{,}54 \\ \varphi_s = 171{,}7° \end{array}\right\} \Longrightarrow \sigma_{so} = 21{,}0\ \text{cm}$$

VII. CONCLUSION

An exact particle tracking in the EPA bending magnet has been able to remove all the approximations and uncertainties of the corresponding beam behaviour in the particular difficult to treat case of a very low bending radius in a specially short combined function magnet.

The computer program launched for this purpose is in fact quite general and is intended to be used by J.P. Riunaud to analyse the future PS wiggler fine characteristics.

Consequently the pole profile and main parameters of the EPA bending magnet could be specified.

Moreover the position of the main EPA lattice clements have been confirmed and the synchrotron integrals dependent parameters modified. It concerns particularly the damping time constants and the beam emittances during accumulation as well as at equilibrium.

The precision of these parameters depends in fact only of the accuracy of the magnetic field estimations. They will easily be refined after the bending magnet magnetic measurement by using the same particle tracking program.

VIII. Acknowledgments :

We would like to emphasize here the extremely close and fruitful collaboration we had with D. Cornuet, without which this work would not have been possible.

The appropriate adaptation by T. Risselada of the optic program AGS enables the fine adjustment of the bending pole profile, thus avoiding undesirable lattice perturbations.

./.

References :

1) J.P. Delahaye, A. Krusche : The LEP Electron Positron Accumulator (E.P.A.) ; Basic parameters and lattice structure, LEP Note 408 and PS/LPI/Note 82-8.

2) D. Cornuet : Calculation of the magnetic field in the EPA bending magnet ; personal communication.

3) J.P. Delahaye : Qualités de champ magnétique requises dans l'aimant de courbure EPA; PS/LPI/Note 82-15.

4) D. Cornuet : Compte rendu de la réunion du 18.3.82 concernant la définition des aimants de l'EPA : PS/PSR/Min. 82-4.

5) J.P. Delahaye : Effect and correction of an integrated focussing error strength in the EPA bending magnets : PS/LPI/Note 83-4.

6) H. Kugler : Evaluation with Patricia of the EPA dynamical acceptance ; To appear

7) M.G.N. Hine : Effect of systematic magnet and momentum error CERN/PS/MGNH/Note 17.

8) P. Bossard, H. Umstatter : Personal communication.

9) D. Cornuet, G. Suberlucq,H. Umstatter : Magnetic measurements of 1 m standard PS magnet and their consequences on EPA bending magnets ; PS/PSR/Min. 82-13.

10) E. Keil and alii ; AGS, the ISR computer program for synchrotron design, orbit analysis and insertion matching, CERN 75-13.

11) P. Pearce : Personal communication.

Annex 1 : Integrated bending and focussing strength in a small bending radius bending magnet.

Let be a magnet of total length, l, in the hard edge approximation, where the magnetic field is given by :

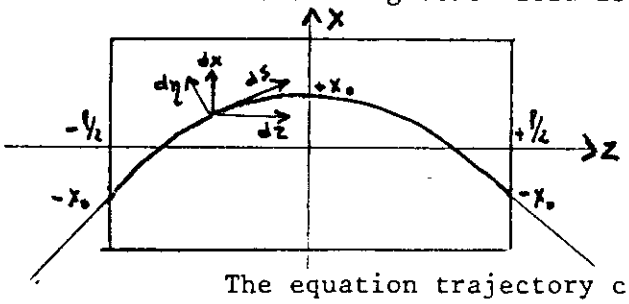

$$B_y = a_1 + a_2 x + a_3 \frac{x^2}{l}$$

The equation trajectory can be approximated by

$$x(z) = 2 x_0 \cos\left(\frac{\pi z}{l}\right) - x_0$$

All along this trajectory :

$$dx = d\eta . \cos\varphi \qquad dz = ds . \cos\varphi$$

$$tg\,\varphi = dx/dz = -\frac{2x_0}{\pi} \sin\left(\frac{\pi z}{l}\right) \qquad \frac{1}{\cos\varphi} \sim 1 + \frac{\varphi^2}{2} \sim 1 + 2\left(\frac{x_0}{\pi}\right)^2 \sin^2\left(\frac{\pi z}{l}\right)$$

The integrated bending strength along the trajectory becomes :

(neglecting the terms of order greater than x_o^2)

$$\int B\,ds = \int a_1 \frac{dz}{\cos\varphi} + \int a_2 x \frac{dz}{\cos\varphi} + \int \frac{a_3}{l} x^2 \frac{dz}{\cos\varphi}$$

$$\int B\,ds \sim a_1 \left[\int dz + 2\left(\frac{x_0}{\pi}\right)^2 \int \sin^2\left(\frac{\pi z}{l}\right) dz \right]$$

$$+ a_2 \left[2x_0 \int \cos\left(\frac{\pi z}{l}\right) dz - x_0 \int dz \right]$$

$$+ a_3 \left[2x_0^2 \int \cos^2\left(\frac{\pi z}{l}\right) dz - 2x_0^2 \int \cos\left(\frac{\pi z}{l}\right) dz + \frac{x_0^2}{l} \int dz \right]$$

$$\int B\,ds \sim a_1 \left[[z]_{-l/2}^{+l/2} + 2\left(\frac{x_0}{\pi}\right)^2 \left\{ \left[\frac{z}{2}\right]_{-l/2}^{+l/2} - \left[\frac{\sin\left(\frac{2\pi z}{l}\right)}{4\,\pi/l}\right]_{-l/2}^{+l/2} \right\} \right]$$

$$+ a_2 \left[2x_0 \frac{l}{\pi} \left[\sin\left(\frac{\pi z}{l}\right)\right]_{-l/2}^{+l/2} - x_0 [z]_{-l/2}^{+l/2} \right]$$

$$+ a_3 \left[2x_0^2 \left\{ \left[z/2\right]_{-l/2}^{+l/2} + \left[\frac{\sin\left(\frac{2\pi z}{l}\right)}{4\,\pi/l}\right]_{-l/2}^{+l/2} - \frac{l}{\pi}\left[\sin\left(\frac{\pi z}{l}\right)\right]_{-l/2}^{+l/2} + \frac{[z]_{-l/2}^{+l/2}}{4} \right\} \right]$$

$$\int B ds \sim a_1 \left[l + \frac{x_0^2 l^3}{2\pi^2} \right] + a_2 \left[4 x_0 \frac{l}{\pi} - x_0 l \right]$$

$$+ a_3 \left[\frac{x_0^2 l}{2} - 4 x_0^2 \frac{l}{\pi} + x_0^2 \frac{l}{2} \right]$$

$$\int B\, ds \sim l \left\{ a_1 \left[1 + \frac{l^2 x_0^2}{2\pi^2} \right] + a_2 x_0 \left[-1 + \frac{4}{\pi} \right] + a_3 x_0^2 \left[1 - \frac{4}{\pi} \right] \right\}$$

$$\boxed{\int B ds \sim l \left[a_1 \left(1 + 0{,}05 l^2 x_0^2 \right) + 0{,}273 a_2 x_0 - 0{,}273 a_3 x_0^2 \right]}$$

The integrated focussing strength perpendicular to the trajectory becomes

$$\int G ds = \int \frac{dB_y}{d\eta} ds = \int \frac{dB_y}{dx} \frac{dx}{d\eta} ds = \int \frac{dB_y}{dx} \frac{\cos\varphi}{\cos\varphi} dz$$

$$\boxed{\int G ds = \int \frac{dB_y}{dx} dz = \int (a_2 + a_3 x)\, dz}$$

$$\int G ds = \int a_2 dz + \int a_3 2 x_0 \cos\left(\frac{\pi z}{l}\right) dz - \int a_3 x_0 dz$$

$$= a_2 \left[z \right]_{-l/2}^{+l/2} + 2 x_0 a_3 \left[\frac{l}{\pi} \sin\left(\frac{\pi z}{l}\right) \right]_{-l/2}^{+l/2} - a_3 x_0 \left[z \right]_{-l/2}^{+l/2}$$

$$= a_2 l + 4 x_0 a_3 \frac{l}{\pi} - a_3 x_0 l$$

$$\boxed{\int G ds = l \left[a_2 + 0{,}273\ a_3 x_0 \right]}$$

Numerical application in the EPA case :

$l = 0.56$ m ; $x_o = 0.0138$ m ; $a_1 = 1.4$ T

then the introduction of the gradient $a_2 = -1$,T/m modifies the total Bdl by 21 gm (- 0.3 %)

In the same way the introduction of a sextupole $a_3 = +1$ T/m^2 would modify

- the total Bdl by 0.3 gm ($- 4 \times 10^{-5}$)
- the total Gdl by 21 g (- 0.4 %)

./.

Annex 2 : Exact differential equations of motion

Let's the magnetic field B expressed by its components in the three planes : B_x, B_y, B_z.

Horizontal movement :

$$m \frac{d^2x}{dt^2} = -e \frac{dz}{dt} B_y + e \frac{dy}{dt} B_z$$

$$m \frac{d^2z}{dt^2} = +e \frac{dx}{dt} B_y - e \frac{dy}{dt} B_x$$

$$\frac{d^2x}{dz^2} = \left(\frac{dt}{dz}\right)^2 \left(\frac{d^2x}{dt^2} - \frac{dx}{dz} \frac{d^2z}{dt^2} \right)$$

$$= \frac{e}{m} \left(\frac{dt}{dz}\right)^2 \left[- \frac{dz}{dt} B_y + \frac{dy}{dt} B_z - \frac{dx}{dz} \left(\frac{dx}{dt} B_y - \frac{dy}{dt} B_x \right) \right]$$

$$= \frac{e}{m} \left(\frac{dt}{dz}\right) \left[- B_y + \frac{dy}{dz} B_z - \frac{dx}{dz} \left(\frac{dx}{dz} B_y - \frac{dy}{dz} B_x \right) \right]$$

$$\boxed{\frac{d^2x}{dz^2} = \frac{e}{p} \sqrt{1 + \left(\frac{dx}{dz}\right)^2 + \left(\frac{dy}{dz}\right)^2} \left\{ - B_y \left[1 + \left(\frac{dx}{dz}\right)^2 \right] + \frac{dy}{dz} \left(B_z + \frac{dx}{dz} B_x \right) \right\}}$$

in case of a movement in the horizontal plane only, this equation can be simplified :

$$\frac{dy}{dz} = 0 \quad \Rightarrow \quad \boxed{\frac{d^2x}{dz^2} = - \frac{e}{p} B_y \left[1 + \left(\frac{dx}{dz}\right)^2 \right]^{3/2}}$$

Vertical movement :

$$m \frac{d^2y}{dt^2} = - e \frac{dx}{dt} B_z + e \frac{dz}{dt} B_x$$

$$m \frac{d^2z}{dt^2} = + e \frac{dx}{dt} B_y - e \frac{dy}{dt} B_x$$

$$\frac{d^2y}{dz^2} = \left(\frac{dt}{dz}\right)^2 \left(\frac{d^2y}{dt^2} - \frac{dy}{dz} \frac{d^2z}{dt^2} \right)$$

$$\frac{d^2y}{dz^2} = \frac{e}{m}\left(\frac{dt}{dz}\right)^2\left[-\frac{dx}{dt}B_z + \frac{dz}{dt}B_x - \frac{dy}{dz}\left(\frac{dx}{dt}B_y - \frac{dy}{dt}B_x\right)\right]$$

$$\frac{d^2y}{dz^2} = \frac{e}{m}\left(\frac{dt}{dz}\right)\left[-\frac{dx}{dz}B_z + B_x - \frac{dy}{dz}\left(\frac{dx}{dz}B_y - \frac{dy}{dz}B_x\right)\right]$$

$$\frac{d^2y}{dz^2} = \frac{e}{m}\left(\frac{dt}{dz}\right)\left\{B_x\left[1+\left(\frac{dy}{dz}\right)^2\right] - \frac{dx}{dz}\left(B_z + \frac{dy}{dz}B_y\right)\right\}$$

$$\boxed{\frac{d^2y}{dz^2} = \frac{e}{p}\sqrt{1+\left(\frac{dx}{dz}\right)^2+\left(\frac{dy}{dz}\right)^2}\left\{B_x\left[1+\left(\frac{dy}{dz}\right)^2\right] - \frac{dx}{dz}\left(B_z + \frac{dy}{dz}B_y\right)\right\}}$$

In case of a movement in the vertical plane only this equation can also be simplified :

$$\frac{dx}{dz} = 0 \Rightarrow \boxed{\frac{d^2y}{dz^2} = \frac{e}{p}B_x\left[1+\left(\frac{dy}{dz}\right)^2\right]^{3/2}}$$

But the complete vertical differential equation has to be used in an horizontal bending magnet because of the simultaneous curvature in the horizontal plane ($dx/dz \neq 0$).

Magnetic field components outside of the mid-plane :

The magnetic field components are usually calculated or measured only in the mid plane. Then for vertical tracking outside of the mid plane, the real magnetic field components have to be deduced from their mid-plane values.

Let the indice o associated with these mid-plane values, the components outside the mid plane can be approximated up to the second order by :

$$B_y(x,y) = B_{y_o} + x\left(\frac{dB_y}{dx}\right)_o + \frac{1}{2}x^2\left(\frac{d^2B_y}{dx^2}\right)_o$$

$$\frac{dB_x}{dy} = \frac{dB_y}{dx} \Rightarrow B_x(x,y) = y\left[\left(\frac{dB_y}{dx}\right)_o + x\left(\frac{d^2B_y}{dx^2}\right)_o\right]$$

$$\frac{dB_z}{dy} = \frac{dB_y}{dz} \Rightarrow B_z(x,y) = y\left\{\left(\frac{dB_y}{dz}\right)_o + x\left[\frac{d}{dz}\left(\frac{dB_y}{dx}\right)\right]_o + \frac{x^2}{2}\left[\frac{d}{dz}\left(\frac{d^2B_y}{dz^2}\right)\right]\right\}$$

T A B L E 1 : Modified parameters of the EPA design

	Symbol	EPA Design PS/LPI 82-8	EPA Design PS/LPI 82-13	New parameter after tracking	% change	Units
BENDING MAGNET						
Central magnetic field	B_0	1,400		1,400	0	T
Central magnetic gradient	$(dBy/dx)_0$	-1,000		-1,120	+12	T/m
Central magnetic sextupole	(d^2By/dx^2)	0		0	0	T/m^2
$\int Bdl$ along the trajectory	$\int Bds$	0,7854		0,7854	0	Tm
$\int Bdl$ along magnet axis	$\int Bdz$	0,7854		0,7846	-0,1	Tm
Bending magnetic length	l_B	561		560,4	0	mm
$\int (dB/dx)dz$ along magnet axis	$\int GdZ$	-0,5610		-0,5452	-3	T
Gradient magnetic length	l_6	561		487	-13	mm
$\int (d^2By/dx^2)dz$ along magnet axis	$\int SdZ$	0		0	0	T/m
Equivalent transfer matrix coefficients	H_{11}	1,0798		1,0786	0	
	H_{12}	0,5617		0,5636	+0,3	
	H_{21}	0,2954		0,2987	-2	
	H_{13}	0,1103		0,1106	0	
	H_{23}	0,4083		0,4078	0	
	V_{11}	0,8540		0,8518	-0,3	
	V_{12}	0,5455		0,5495	+0,7	
	V_{21}	-0,4962		-0,4993	+0,6	
Synchrotron integrals	I_1	4,1750		4,1731	0	
	I_2	4,4060		3,9497	-10	
	I_3	3,0900		2,6379	-14,6	
	I_4	-4,2590		-3,9803	-6,5	
	I_5	2,3620		2,0165	-17,6	
LATTICE						
Betatron tune	Q_x	4,45		4,45	0	-
	Q_y	4,38		4,38	0	-
Normalized transition energy	γ_{tr}	5,52		5,54	+0,3	-
Twiss parameters	$\beta_x max$	14,9		14,9	0	m
	$\beta_y max$	14,4		14,2	-1,4	m
	$D_x max$	2,29		2,27	-0,9	m
	$D_x min$	0		0	0	m
BEAM DYNAMICS						
Energy loss per turn	U_γ	8,04		7,21	-10	keV
Stable phase angle (V_{RF} = 50 kV)	ϕ_s	170,7°		171,7°	+0,6	degrés
Damping partition number	J_x	1,97		2,01	+2	
	J_y	1		1	0	
	J_ε	1,03		0,99	-4	
Damping time constants	τ_x	31,81		34,75	+9,3	msec
	τ_y	62,57		69,77	+11,5	msec
	τ_ε	60,55		70,33	+16,1	msec
Beam emittances ($\pm 1\ \sigma$) after injection	ε_T	108		119	+10	$\pi\mu$radm
at equilibrium	ε_{xo}	0,144		0,135	-6,2	$\pi\mu$radm
(κ_x=0; κ_y=0.25)	ε_{yo}	0,029		0,027	-7	$\pi\mu$radm
Momentum dispersion at equilibrium	σ_E/E	6,07		5,98	-1,5	10^{-4}
Bunch length at equilibrium	σ_{so}	21,6		21,0	-2,8	cm

EPA:VERSION 83/07) PS PS 75.03 28/07/83 15.40.40

CIRCUMFERENCE = 125.66680 2 HALF SUPERPERIODS STRAIGHT MAGNETS ALL VALUES AT EXIT OF ELEMENTS

NO	ELEM		L(M)	ANG(MR)	K(1/M2)	BETAV(M)	BETAH(M)	ALPHAV	ALPHAH	MUV/2PI	MUH/2PI	ALPHAP(M)	ALPHAP'
INITIAL						3.130	14.258	0.000	0.000	0.00000	0.00000	-.000	-.000
1	L1		2.9285	0.0000	0.0000000	5.870	14.860	-.936	-.205	.11970	.03224	-.000	-.000
2	F1/2		.1900	0.0000	-1.0967076	6.402	14.358	-2.329	2.813	.12464	.03430	-.000	.000
3	F1/2		.1900	0.0000	-1.0967076	7.687	12.778	-4.095	5.392	.12895	.03652	-.000	.000
4	L2		.4602	0.0000	0.0000000	11.946	8.314	-5.159	4.309	.13660	.04362	-.000	.000
5	B1	18.3	.5636	392.7000	.8518054	14.196	5.180	1.671	1.688	.14331	.05731	.111	.408
6	L2		.4602	0.0000	0.0000000	12.714	3.784	1.548	1.346	.14877	.07388	.298	.408
7	FC/2		.1500	0.0000	-.0284053	12.264	3.395	1.456	1.249	.15068	.08054	.359	.406
8	FC/2		.1500	0.0000	-.0284053	11.840	3.035	1.368	1.149	.15266	.08798	.420	.405
9	LJ		.8960	0.0000	0.0000000	9.584	1.590	1.150	.464	.16606	.15484	.783	.405
10	SD		.3000	0.0000	0.0000000	8.916	1.381	1.078	-.235	.17123	.18728	.904	.405
11	L2		.4602	0.0000	0.0000000	7.975	1.327	.966	-.117	.17992	.24250	1.091	.405
12	B1	18.3	.5636	392.7000	.8518054	4.955	1.928	3.715	-1.034	.19385	.29982	1.515	1.160
13	L2		.4602	0.0000	0.0000000	2.169	3.107	2.340	-1.528	.21626	.32992	2.049	1.160
14	F2/2		.1900	0.0000	-1.3892226	1.470	3.553	1.401	-.781	.23338	.33895	2.217	.595
15	F2/2		.1900	0.0000	-1.3892226	1.068	3.681	.747	.119	.25781	.34724	2.273	.000
16	LS		.3625	0.0000	0.0000000	.719	3.631	.218	.019	.32569	.36305	2.273	.000
17	SF		.3000	0.0000	0.0000000	.719	3.644	-.219	-.063	.39421	.37619	2.273	.000
18	LS		.3625	0.0000	0.0000000	1.069	3.726	-.748	-.163	.46205	.39187	2.273	.000
19	F2/2		.1900	0.0000	-1.3892226	1.471	3.612	-1.402	.753	.48645	.40005	2.217	-.595
20	F2/2		.1900	0.0000	-1.3892226	2.171	3.173	-2.342	1.521	.50355	.40891	2.049	-1.160
21	L2		.4602	0.0000	0.0000000	4.959	1.994	-3.717	1.041	.52595	.43820	1.515	-1.160
22	B1	18.3	.5636	392.7000	.8518054	7.981	1.386	-.966	.122	.53987	.49325	1.091	-.405
23	L2		.4602	0.0000	0.0000000	8.921	1.429	-1.078	-.215	.54855	.54627	.904	-.405
24	SD		.3000	0.0000	0.0000000	9.590	1.623	-1.150	-.434	.55372	.57783	.783	-.405
25	LJ		.8960	0.0000	0.0000000	11.846	2.989	-1.367	-1.090	.56711	.64450	.420	-.405
26	FC/2		.1500	0.0000	-.0284053	12.269	3.331	-1.456	-1.186	.56909	.65207	.360	-.406
27	FC/2		.1500	0.0000	-.0284053	12.720	3.701	-1.548	-1.279	.57100	.65887	.298	-.408
28	L2		.4602	0.0000	0.0000000	14.201	5.028	-1.671	-1.606	.57645	.67588	.111	-.408
29	B1	18.3	.5636	392.7000	.8518054	11.949	8.029	5.162	-4.135	.58317	.69002	.000	.000
30	L2		.4602	0.0000	0.0000000	7.668	12.312	4.097	-5.172	.59081	.69739	.000	.000
31	F1/2		.1900	0.0000	-1.0967076	6.483	13.825	2.330	-2.687	.59513	.69969	.000	.000
32	F1/2		.1900	0.0000	-1.0967076	5.871	14.300	.937	.218	.60006	.70183	.000	.000
33	L1		2.9285	0.0000	0.0000000	3.128	13.649	.009	.004	.71982	.73544	.000	.000
34	L6		.7415	0.0000	0.0000000	3.303	13.683	-.237	-.050	.75687	.74408	.000	.000
35	F3/2		.1950	0.0000	-.5218310	3.475	13.436	-.650	1.312	.76607	.74636	.000	.000
36	F3/2		.1950	0.0000	-.5218310	3.817	12.674	-1.115	2.570	.77462	.74873	.000	.000
37	L7		2.3625	0.0000	0.0000000	12.368	3.880	-2.504	1.152	.83049	.80342	.000	.000
38	D/2		.1950	0.0000	.5236789	13.109	3.525	-1.272	.679	.83292	.81185	.000	.000
39	D/2		.1950	0.0000	.5236789	13.347	3.343	-.061	.259	.83525	.82092	.000	.000
40	LB/2		.8115	0.0000	0.0000000	13.297	3.133	-.000	.000	.84496	.86126	.000	.000
41	LB/2		.8115	0.0000	0.0000000	13.347	3.343	-.061	-.259	.85466	.90160	.000	.000
42	D/2		.1950	0.0000	.5236789	13.110	3.524	1.272	-.678	.85699	.91068	.000	.000
43	D/2		.1950	0.0000	.5236789	12.368	3.879	2.504	-1.152	.85942	.91910	.000	.000
44	L9		1.5225	0.0000	0.0000000	6.106	8.778	1.609	-2.065	.88745	.96112	.000	.000
45	QB/2		.1900	0.0000	0.0000000	5.516	9.584	1.497	-2.179	.89266	.96441	.000	.000
46	QB/2		.1900	0.0000	0.0000000	4.968	10.434	1.386	-2.293	.89844	.96744	.000	.000
47	L2		.4602	0.0000	0.0000000	3.817	12.672	1.115	-2.570	.91529	.97381	.000	.000
48	F3/2		.1950	0.0000	-.5218310	3.475	13.434	.650	-1.311	.92385	.97618	.000	.000
49	F3/2		.1950	0.0000	-.5218310	3.303	13.681	.237	-.051	.93304	.97846	.000	.000
50	L6		.7415	0.0000	0.0000000	3.128	13.647	-.000	-.004	.97009	.98710	.000	.000
51	L6		.7415	0.0000	0.0000000	3.304	13.693	-.237	-.050	1.00713	.99574	.000	.000
52	F3/2		.1950	0.0000	-.5218310	3.476	13.448	-.651	1.305	1.01033	.99802	.000	.000
53	F3/2		.1950	0.0000	-.5218310	3.818	12.688	-1.116	2.565	1.02488	1.00039	.000	.000
54	L7		2.3625	0.0000	0.0000000	12.373	3.902	-2.505	1.154	1.08072	1.05488	.000	.000
55	D/2		.1950	0.0000	.5236789	13.115	3.547	-1.272	.678	1.08315	1.06326	.000	.000
56	D/2		.1950	0.0000	.5236789	13.352	3.366	.061	.257	1.08549	1.07228	.000	.000
57	LB/2		.8115	0.0000	0.0000000	13.303	3.157	.000	-.000	1.09518	1.11232	.000	.000

DP/P	COSMU(H)	Q(H)	QPRIME(H)	BETAMAX(H)	COSMU(V)	Q(V)	QPRIME(V)	BETAMAX(V)	XMAX(H)	GAMMA TR.
0.0000	.15874	4.4493	0.0000	14.8597	.36597	4.3807	0.0000	14.2013	2.2733	5.5393

DP/P = 0.0000 AVERAGE X = 0.0000 AVERAGE ALPHAP = .6518 R.F. GAMMA TR. = 5.5303

Table 2: AGS listing of the EPA lattice including the calculated bending magnet equivalent transfer matrix.

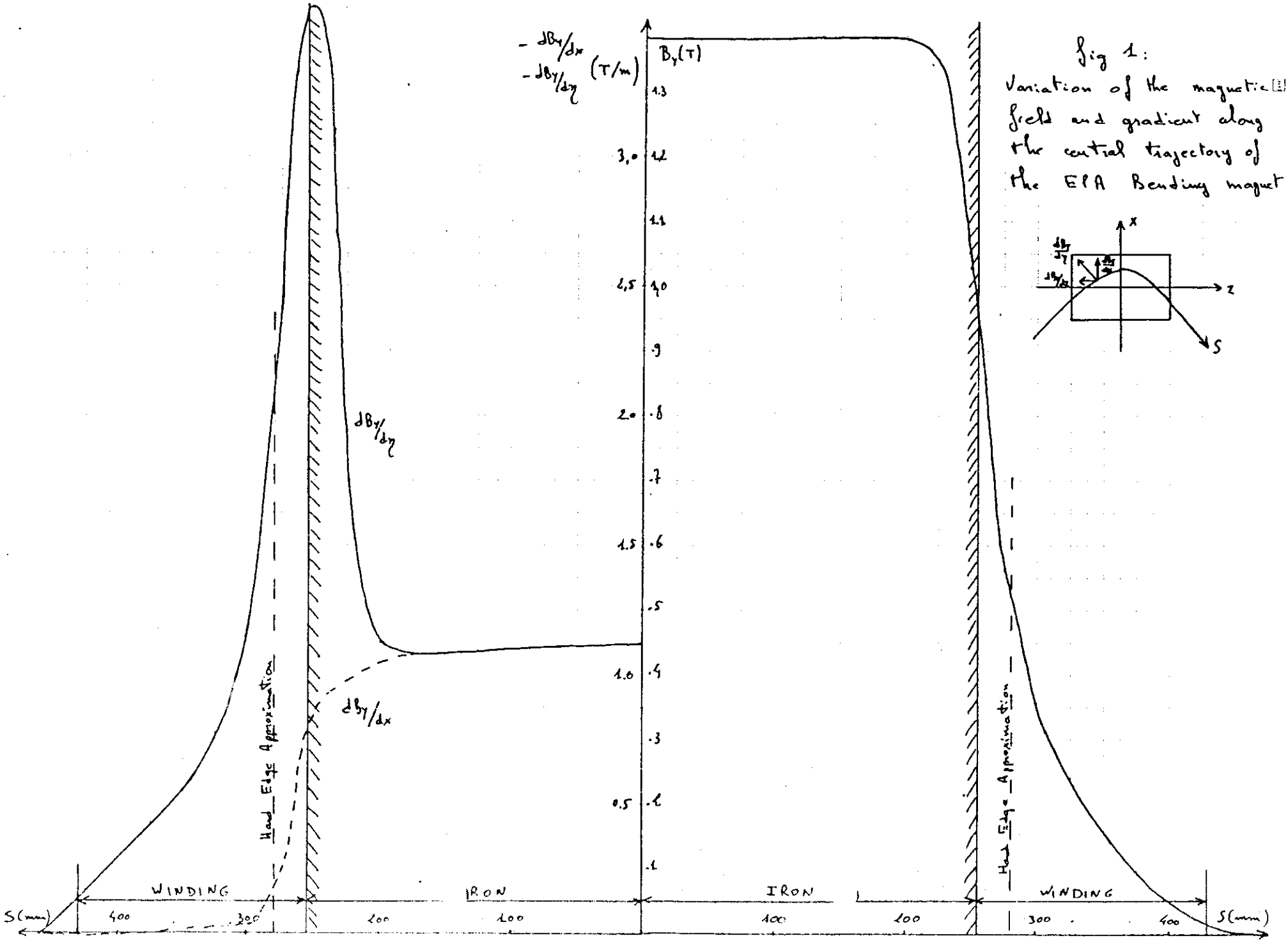

Fig 1:
Variation of the magnetic field and gradient along the central trajectory of the EPA Bending magnet

Fig 2: Perturbation of the EPA working point by different gradient field configurations in the bending magnets

Case	$G_0 = dB_y/dx$	$\int G dz$
①	− 1,124 T/m	− 0,554 T
②	− 1,104 T/m	− 0,536 T
③	− 1,114 T/m	− 0,550 T
④	− 1,120 T/m	− 0,545 T

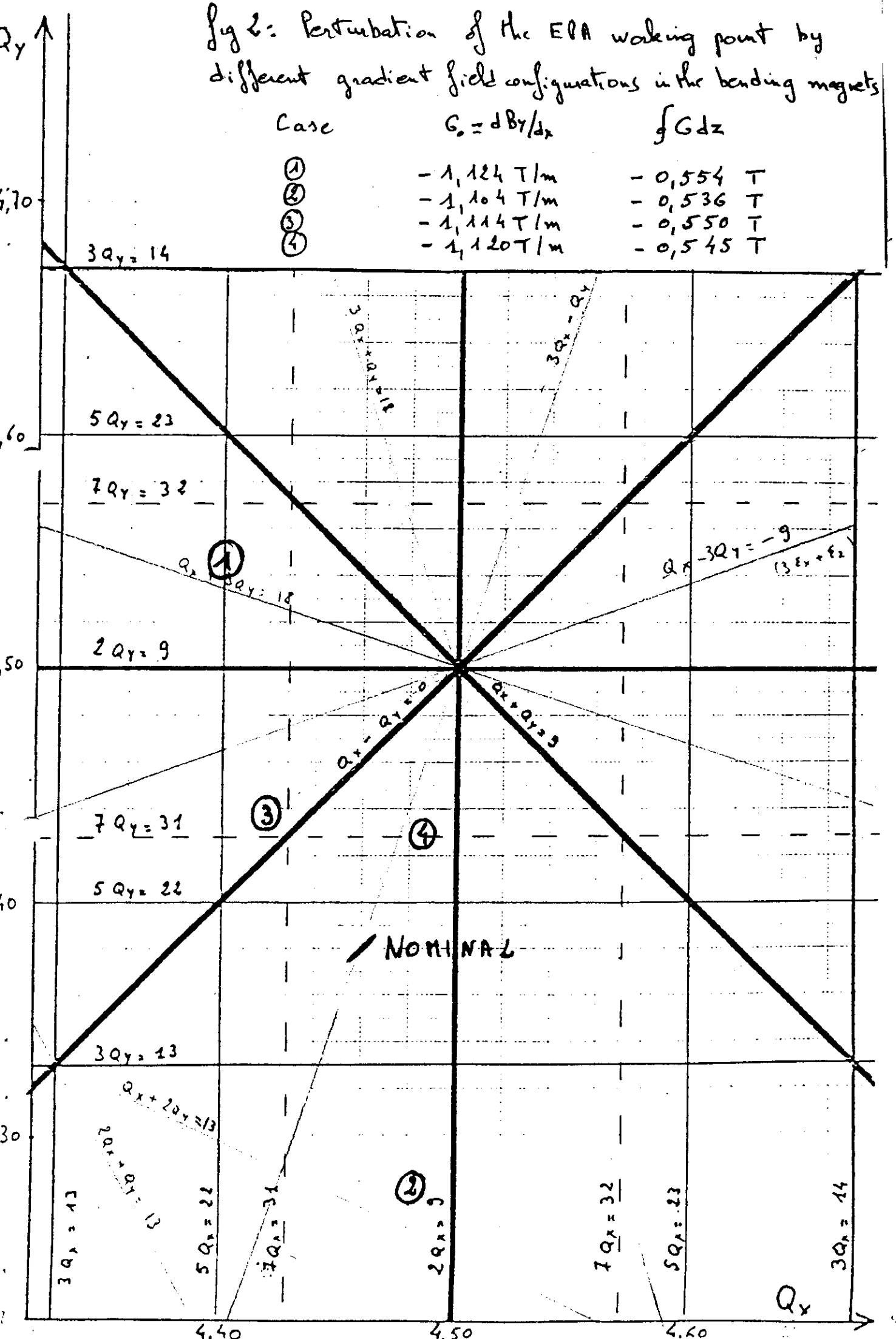

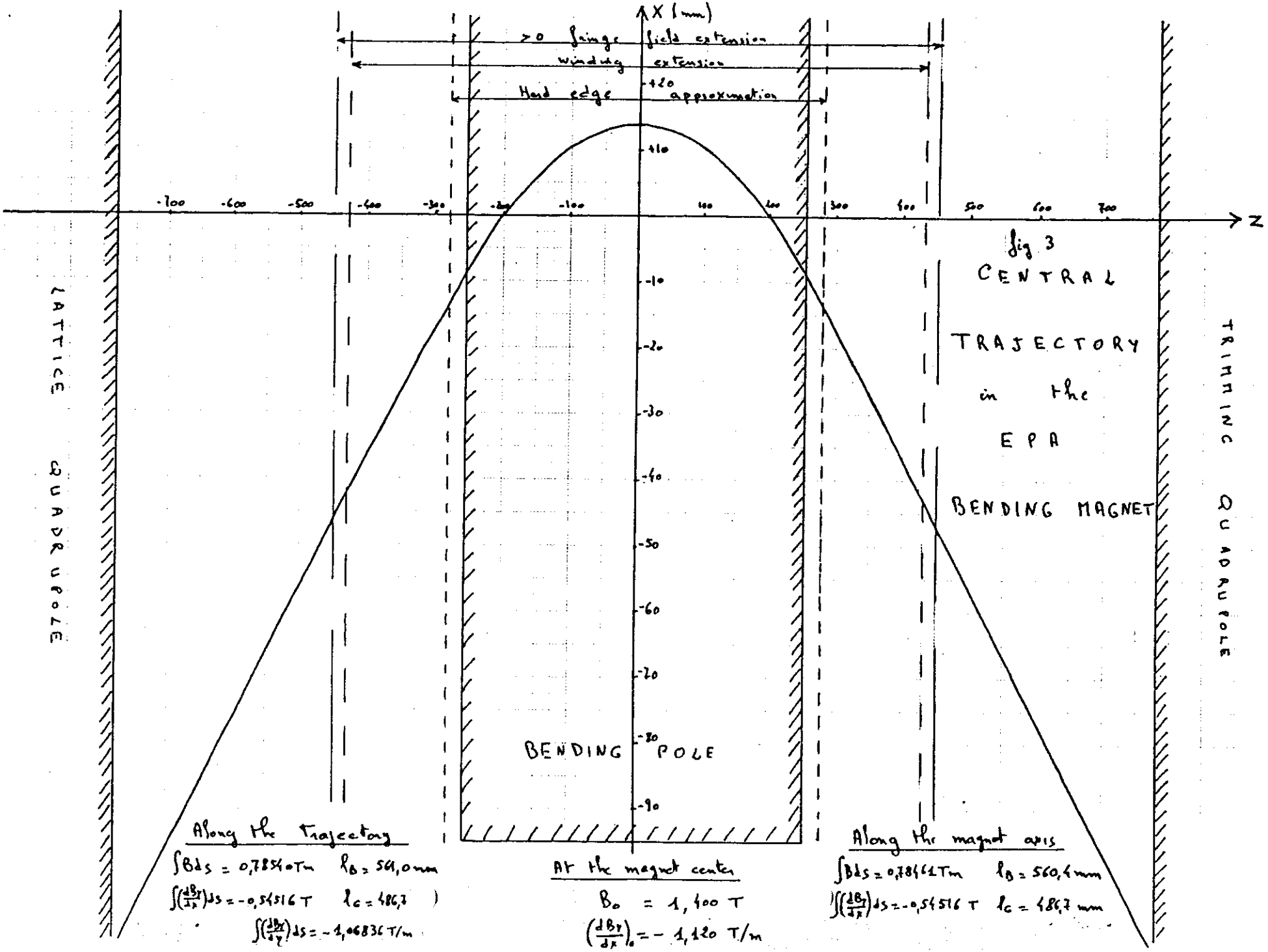
X (mm)
> 0 fringe field extension
winding extension
Hard edge approximation
+120
+10
-10
-20
-30
-40
-50
-60
-70
-80
-90
-100
-600
-500
-400
-300
-200
100
200
300
400
500
600
700
Z
LATTICE QUADRUPOLE
TRIMMING QUADRUPOLE
BENDING POLE
CENTRAL TRAJECTORY in the EPA BENDING MAGNET
Along the Trajectory
∫Bds = 0,7854 Tm l_B = 541,0 mm
∫(dBy/dx)ds = -0,54516 T l_c = 486,7
∫(dBy/dy)ds = -1,06836 T/m
At the magnet center
B_o = 1,400 T
(dBy/dx)_o = -1,120 T/m
Along the magnet axis
∫Bds = 0,7854 Tm l_B = 560,4 mm
∫(dBy/dx)ds = -0,54516 T l_c = 486,7 mm

fig 3